Piotr Śliwiński, Marek St. Węglowski, Krzysztof Kwieciński, Andrzej Wieczorek

Electron Beam Surface Hardening

Abstract: The surface hardening of steel components makes it possible to achieve high abrasive wear resistance without the necessity of hardening the entire cross-section of a given element. As a result, lower stress are introduced and the cost of the process can be reduced. Because of very high heating rates (of up to 10^9 K/s) as well as the ease of dynamic deflection and focusing, the use of the electron beam to harden component surfaces enables the obtainment of surface layers characterised by required properties. This article constitutes an overview of publications concerning electron beam-based surface hardening.

Keywords: hardening, surface hardening, case hardening, electron beam, surface processing, steel

DOI: *10.17729/ebis.2022.1/1*

Introduction

Since antiquity, hardening has been used to increase the wear resistance, hardness and plastic strain resistance of various elements. Gradually, along with advancements made in their production, iron alloys have been characterised by increasingly low contents of carbon. In spite of the fact that the aforesaid alloys were characterised by high plasticity and workability, they could not be used to make tools or weapons and, in addition, were characterised by low hardenability. The first surface processing method aimed to obtain hard surface without compromising favourable plastic properties was carbonizing, also referred to as case hardening. The abovenamed process, where the surface layer of an element is provided (through diffusion) with carbon atoms, increases the mechanical properties of iron alloys. Until the 20th century, case hardening was the only method enabling the obtainment of the hard and wear resistant surface layer of steels or cast steels [1–3]. The soft and plastic core combined with the resistant surface layer provide numerous advantages. Materials characterised by high plasticity are also characterised by high workability and formability, which leads to reduced manufacturing costs. In addition, the low hardness of surface before hardening facilitates machine cutting, making the process less laborious and expensive [4–9].

Upper layers are, by convention, divided into coatings and surface layers. The coating is a layer made or applied on the metallic surface in a natural or artificial way, whereas the surface layer constitutes the material surface and the subsurface area, the properties of which differ from those of layers located deeper in the material [4–7]. The division of methods used in the fabrication of surface layers is presented in Figure 1.

mgr inż. Piotr Śliwiński, dr inż. Marek St. Węglowski, mgr inż. Krzysztof Kwieciński – Łukasiewicz Research Network – Instytut Spawalnictwa, Research Group for Materials Weldability and Welded Structures; dr hab. inż. Andrzej Wieczorek – Silesian University of Technology

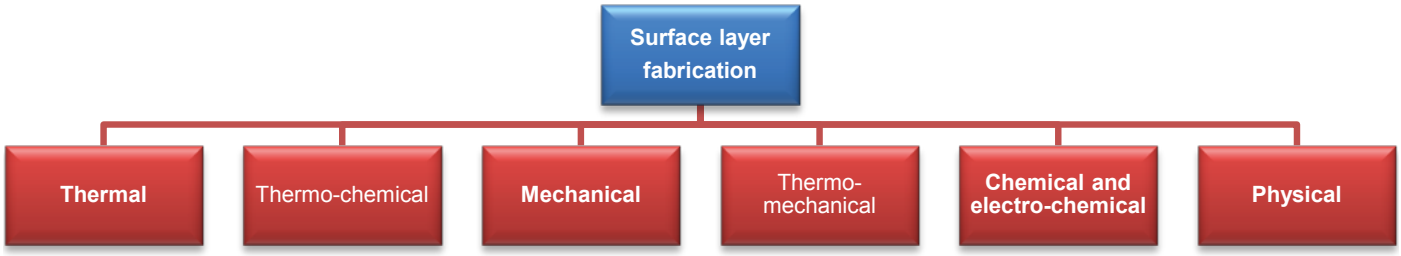

Fig 1. Methods used to obtain surface layers [7]

Presently, there are many methods enabling the fabrication of surface layers on elements made of iron alloys. One of such processes is surface hardening, i.e. a heat processing method consisting in the heating of the surface layer of a given element by 30–50 K above the austenitisation temperature and ensuring the sufficiently fast discharge of heat so that the martensitic or bainitic transformation could take place. The hardening of the surface layer reduces stresses and strains, the consumption of energy and, consequently, manufacturing costs. In terms of the presence or absence of the liquid phase during the process, surface hardening can be divided into hardening with and without melting [4–9].

Surface hardening methods can be divided into [8,9]:

- flame hardening,
- induction hardening,
- quench hardening,
- laser hardening,
- electron beam hardening,
- contact hardening, and
- electrolytic hardening.

Electron beam hardening

Electron beam hardening is a process using the electron beam as the source of energy. The process involves the excitation and emission of electrons from the cathode, usually made of tungsten or a tungsten alloy. Electrons are first accelerated using very high voltage (even 300 kV) and, next deflected and directed to the working chamber using electromagnetic coils [10–13]. The design of the electron gun is presented in Figure 2.

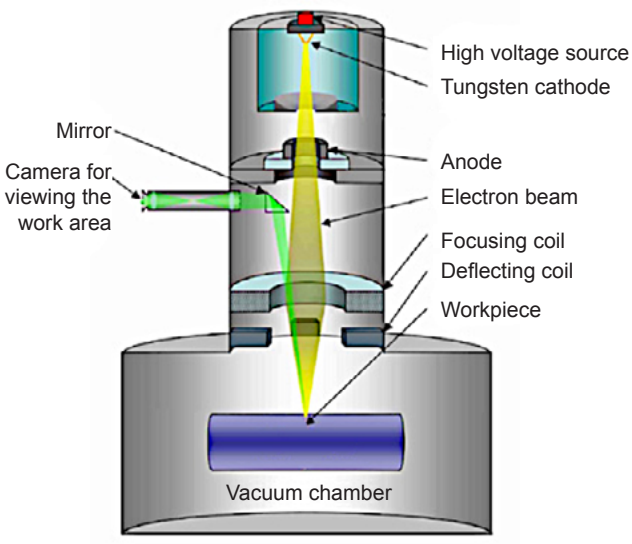

Fig. 2. Electron gun and its components [14, 15]

The beam of electrons "bombards" and, through changing kinetic energy into thermal one, increases the temperature of the surface of a given material. The proportion of the mass subjected to electron beam hardening to the mass not subjected to hardening should be low enough for the latter to absorb heat from the surface. The above-named absorption should be fast enough to exceed the critical rate and enable the martensitic or bainitic transformation [10, 12, 18–20].

Electron beam machines can be divided in relation to applied voltage (into low-voltage, i.e. up to 60 kV and high-voltage devices, i.e. above 60 kV, devices), vacuum level (with high vacuum, i.e. above 10^{-4} mbar, medium vacuum, i.e. above 10^{-2} mbar, partial vacuum and vacuum-free) and the type of the working chamber (chamber, stroke, lock and mixed). The vacuum level significantly affects process efficiency (growing along with the increasing vacuum level). Because of the interaction of beam electrons with those of the atmosphere, vacuum-free

devices are characterised by low energy conversion efficiency and the limited range of operating distances. However, high vacuum is more difficult to achieve, which extends auxiliary time connected with the exchange of elements being processed in the chamber. The easy change of focusing current and the dynamic deflection of the beam enable the performance of the hardening process using both the focused and defocused electron beam, in the continuous, pulsed or continuously oscillating deflected mode (dynamic, scanning). The shape of oscillation is freely programmable, which facilitates the precise hardening of selected surfaces [10, 18–20]. Figure 3 presents exemplary electron beam scanning related to various oscillation frequencies. Figure 4 contains a schematic diagram of the electron beam hardening process.

The parameters of the electron beam hardening process are as follows:

– accelerating voltage, U [kV],
– beam current, I [mA],
– workpiece travel rate in relation to the electron gun, v [m/s],
– focusing current, If [mA],
– cathode heater current (as regards the directly heated cathode), Ic [A],
– type of oscillation and beam deflection frequency, f [Hz],
– vocal length, l [mm],
– vacuum level, p [mbar].

The primary advantages of electron beam hardening [10, 12, 13, 18–20] are the following:

– metallurgical purity of the process (performed in vacuum),
– precise computer-controlled deflection and focusing of the beam,
– higher (in comparison with other technologies) heating rates (of up to 109 K/s), where the heating of the surface of an element is faster than its heat absorbability (resulting from the heat conductivity of a given material),
– precise adjustment of process parameters,
– high process repeatability,
– easy automation,
– high process precision,
– high energy conversion efficiency (exceeding 90%).

Exemplary applications of the electron beam surface hardening process are presented in Table 1. Figure 5 presents a cam unit hardened using the electron beam.

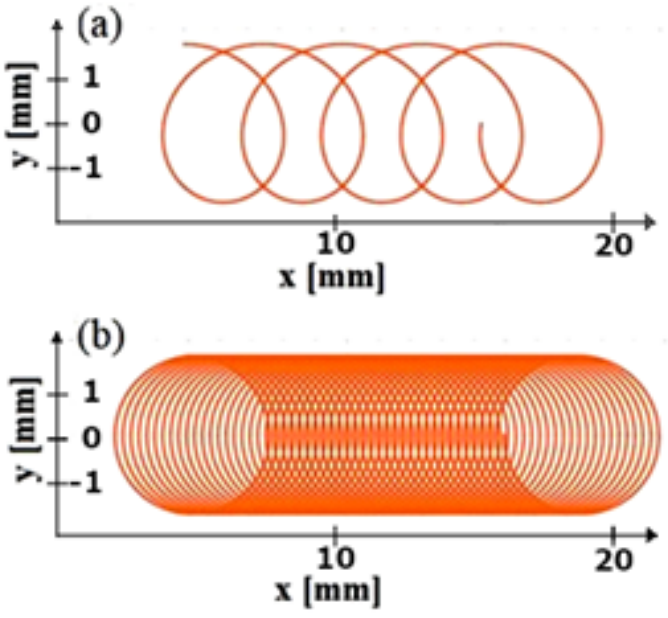

Fig. 3. Exemplary scanning with the electron beam: a) in relation to low oscillation frequency and b) in relation to low oscillation frequency [10, 16]

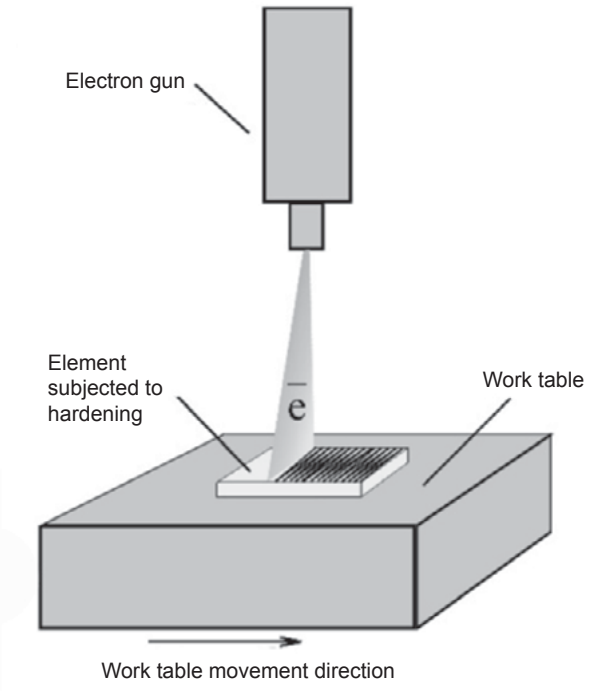

Fig. 4. Schematic diagram of the hardening process with the scanning electron beam [17]

Table 1. Exemplary applications of the electron beam hardening process in relation to the geometry of surface subjected to hardening [19]

Surface geometry	Exemplary applications
Flat surfaces	• guiding rails and work support blades, backing plates and gripping jaws, fasteners, lathe benches
Cylindrical elements • circumference • front surfaces	• spindle guide bushings, drive shafts, guiding bars, rollers, rings, drawing plates and drums, bolts, casting moulds, rotating bushes, crankshafts, brake drums, threaded rings, pivot rims, etc., • pressure rings, retaining rings, valve rings, clamping bolts
Two-dimensionally curved areas	• disk cams, worm gears, screw extruder worms, parts of locks, glass moulds and profiles
Tools and parts of tools	• shear punches, perforated plates, knife-edges, abrasive disks, hammer cutters, blade cutters, drills, milling cutters, lathe tools, metal blades, striking edges

Fig. 5. Set of cams hardened using the electron beam; surface hardness >650 HV, hardness depth >0.4 mm [21]

Study overview

Because of the significant number of modifiable parameters, many research works focus only on results in the form of resultant surface hardness and the hardened layer depth as well as on the simulation and optimisation of the hardening process. It is also of key importance to identify the direct effect of changes of specific parameters on the course and results of the hardening process. Publication [22] discusses tests concerning the effect of various beam deflection modes on the properties of electron beam-hardened layers; the tests were performed using a Probeam K26 machine. The material used in the tests was steel, the chemical composition of which included 0.41% C, 0.69% Mn, 0.25% Si, 1.04% Cr and 0.20% Mo. The patterns of deflection modes involved a single point, a line perpendicular to the direction of movement and composed of 6, 11 and 1000 points respectively (linear mode) as well as a filled field having the shape of a rectangle and a meander. Figure 6 presents process parameters changed during the tests. Figure 7 presents the schematic diagram of the hardening process in the meander-shaped deflection mode.

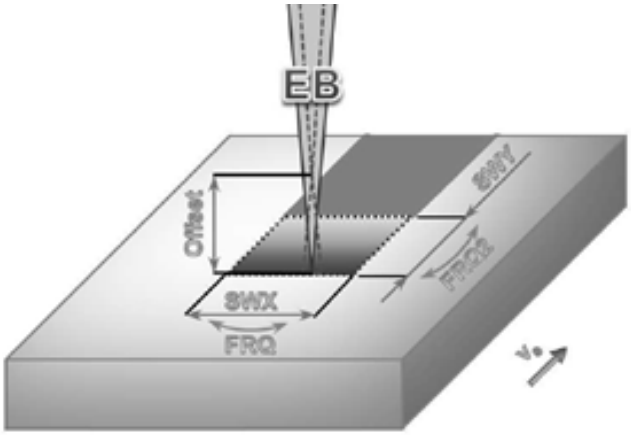

Fig. 6. Schematic diagram presenting parameters of the electron beam hardening process; SWX – amplitude of oscillation perpendicular to the direction of movement [mm]; SWY – amplitude of oscillation parallel to the direction of movement [mm]; Offset – offset of the beam focus in relation to the element surface; FRQ – frequency of oscillation in the direction perpendicular to the direction of movement [Hz] and FRQ2 – frequency of oscillation in the direction parallel to the direction of movement [Hz] [22]

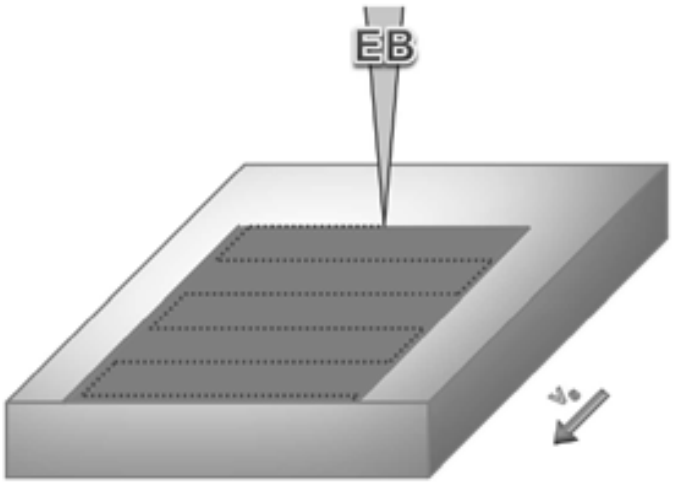

Fig. 7. Electron beam trajectory during meander-shaped deflection [22]

In relation to each pattern (except for the 1-point mode), the amplitude of oscillation (SWX) amounted to 10 mm. Parameters used during the technological tests were optimised in relation to electron beam current I_{EB}. Optimum conditions of energy density were identified experimentally by observing melted areas on the specimen surface. The length of field deflection (SWY) was determined on the basis of the pyrometric measurement of temperature distribution in the beam-affected area. The tests revealed that the deflection mode could affect numerous properties of beads. The greatest grain growth was observed in relation to full circle-shaped oscillation. At the same time it was observed that the deflection mode only slightly affected the maximum hardness. The highest hardness, amounting to 740 HV0.5, was obtained in specimens subjected to hardening performed using the 1-point mode and the meander-shaped deflection mode. Hardness values obtained using the remaining modes were close to 700 HV0.5. It was revealed that the cross-sectional geometric profiles in the beads differed in relation to applied deflection modes. The borderline of the heat affected zone in relation to 6-point, 11-point, linear and meander-shaped mode was parallel to the surface. In the 1-point mode and in the full field mode the above line was significantly curved. The widths of beads were similar (except those obtained using the 1-point mode). The depths of the hardened layers were restricted within the range of 0.1 mm to 1.5 mm. The shallowest depth was obtained in relation to the 1-point mode, whereas the greatest depth was obtained using the field mode. The authors indicated that the hardening rate only affected the depth of the hardened layer (which grew slightly along with the decreasing rate). An increase in focusing current led to an increase in the width of the hardened layer. Overly low values led to significant geometry deformation, whereas excessively high values reduced the hardness of the layers and eliminated the geometrical differences between the applied oscillation modes. Figure 8 presents the effect of the deflection mode and focusing current on the geometry of hardened layers.

Electron beam hardening was also the subject of another publication [23], the authors of which presented results concerning the optimisation of the hardening process involving the use of the oscillating electron beam. The tests involved the use of steel containing 0.42% C, 0.96% Cr, 0.6% Mn and 0.37% Si. The applied mathematical model enabled the calculation of the effect of the specimen travel rate and of the

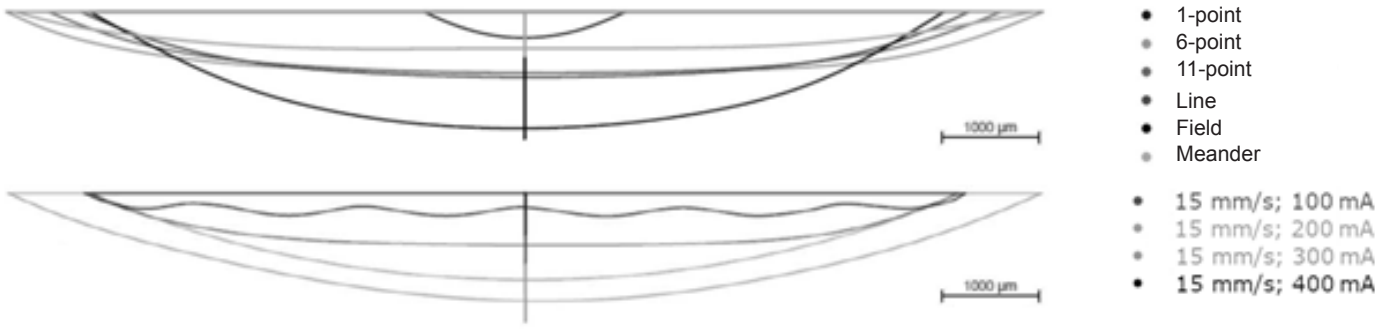

Fig. 8. Effect of deflection modes and beam focusing current on the geometry of hardened layers [22]

beam power on the heating and cooling rates. The tests revealed that the heating rate grew along with the travel rate (in relation to constant electron beam power Q = 3 kW). In relation to rates exceeding 3 cm/s, the heating rate was close to the limit value, where the further increase in the specimen travel rate only slightly affected the heating rate. In addition, the heating rate grew slowly along with an increase in electron beam power (in relation to the constant specimen travel rate). Figure 9 contains a diagram presenting the effect of the specimen travel rate on the heating rate.

The calculations also revealed that the cooling rate was only slightly dependent on electron beam power (in relation to the constant travel rate), yet it was strongly dependent (Fig. 10) on the hardened surface travel rate in relation to the oscillating electron beam.

The results of experimental tests (Fig. 11) revealed the lack of correlation between microhardness and the cooling rate within the range of 2×10^4 K/s to 5×10^4 K/s.

The authors indicated that microhardness changes could be expected in relation to significantly higher cooling rates restricted within the range of 107 K/s to 109 K/s, typical of the pulsed electron beam hardening process. The numerical calculations revealed that the heating and cooling rates as well as the general efficiency of the electron beam hardening process increased along with the increasing travel rate of the specimen [23].

Article [24] discusses tests concerning the optimisation of the electron beam hardening process, involving the performance of the mathematical simulation of the effect of electron process parameters on the microstructure, depth and properties of hardened layers. The simulation was followed by the performance of technological tests involving actual elements. The material used in the tests was steel containing 0.52–0.60% C, 0.50–0.80% Mn, 0.17–0.37% Si, max. 0.040% P, max. 0.040% S, max. 0.25% Cr, max. 0.25% Ni and max. 0.25%

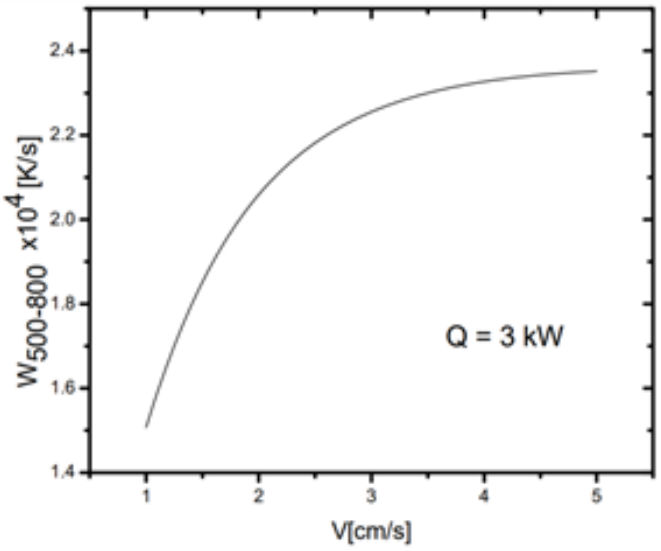

Fig. 9. Calculated effect of the specimen travel rate on the heating rate [23]

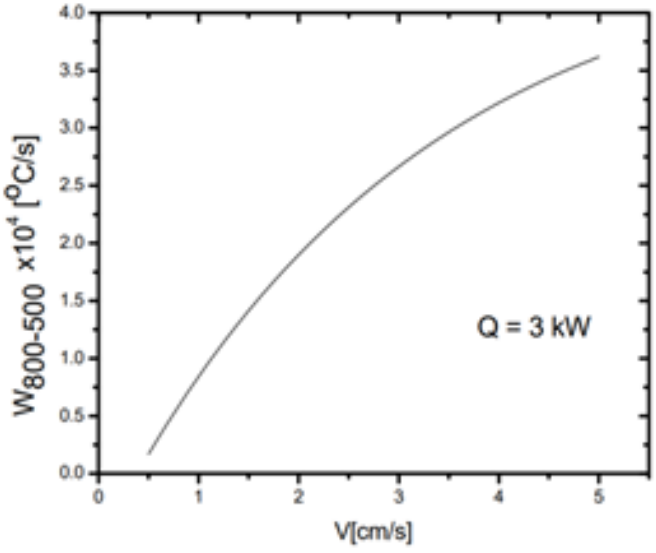

Fig. 10. Calculated effect of the specimen travel rate on the resultant cooling rate [23]

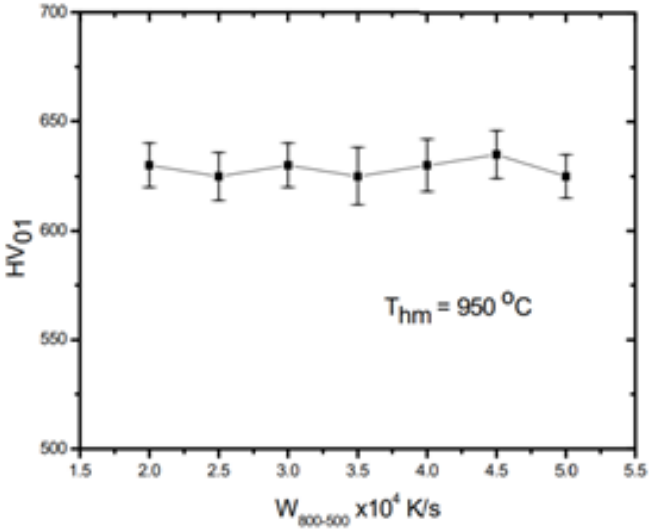

Fig. 11. Experimentally measured effect of the cooling rate on the maximum microhardness of the hardened layers, where T_{hm} = 950°C [23]

Cu. The specimens were subjected to hardening performed using the dynamically deflected electron beam (oscillating); the amplitude of oscillation amounted to 10 mm, whereas the frequency of oscillation amounted to 800 Hz, 1200 Hz and 1600 Hz. The process was performed in relation to an acceleration voltage of 54 kV, 60 kV and 66 kV as well as a beam power of 0.8 kW, 1.1 kW and 1.4 kW (in relation to applied values of accelerating voltage respectively). The depth of the hardened beads obtained in the tests was restricted within the range of 0.3 mm to 1.1 mm, whereas their hardness amounted to as many as 60 HRC. Both the results of the mathematical simulation and those of experimental tests revealed that the applied method of process simulation enabled the identification of the most important factors and of the most favourable hardening conditions within the selected range of parameters. The cooling rate and, consequently, the hardness of the surface were primarily affected (in terms of parameters subjected to analysis) by resultant electron beam power. In turn, hardening depth depended on electron beam energy density on the surface of an element subjected to hardening. However, the authors of publication [23] demonstrated that the cooling rate was primarily affected by the process rate. The authors of publication [24] stated that it was impossible to assess the depth and the homogeneity of the hardened layer as well as to determine the most suitable processing parameters solely on the basis of measurements concerning the average value of surface hardness. The foregoing indicates the necessity of performing metallographic tests and detailed geometrical analysis.

Publication [25] presents the effect of electron beam hardening on the structure and hardness of tool steel AISI D3 (DIN 1.2080, ISO X210Cr12). The tests were performed using the dynamically deflected electron beam (scanning), an accelerating voltage of 60 kV, a current of 5 mA and a hardening rate of 0.6 m/min, 1.2 m/min and 1.8 m/min. The application of the above-presented parameters enabled the making of surface layers having an approximate depth of 400 μm. The highest hardness of the subsurface layer (of approximately 1400 HV0.1) was obtained in relation to the specimen hardened at the highest rate, whereas the lowest hardness (below 1000 HV0.1) was obtained in relation to the specimen hardened at the lowest rate. The hardness of the base material amounted to 650 HV0.1. All of the specimens contained the interlayer having a lowered hardness of approximately 400 HV0.1. The hardness distribution of all the specimens is presented in Figure 12.

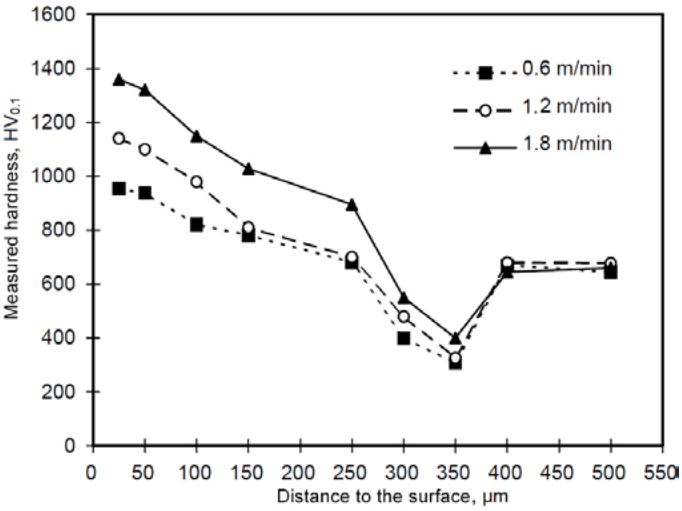

Fig. 12. Hardness distribution in the electron beam-hardened specimens in relation to various hardening rates [25]

The electron beam hardening [26] of nitride steel containing 0.42% C, 0.96% Cr, 0.6% Mn and 0.37% Si enabled the obtainment of a surface layer characterised by a hardness of nearly 850 HV0.1. The above-presented hardness was by approximately 200 HV0.1 higher than that of the nitride layer (amounting to 630 HV0.1) and by 500 HV0.1 than the hardness of the base material (being less than 300 HV0.1). The electron beam having a power of 3 kW was deflected at a frequency of 10 kHz and an amplitude of 14 mm. The deflection of the beam was perpendicular to the direction of the specimen movement. Hardening rates were restricted within the range of 0.5 cm/s to 5 cm/s. During the experiments, the beam focal point was located

above the specimen surface so that the electron beam diameter on the surface amounted to 0.5 mm.

Tests concerning the usability of electron beam hardening in the automotive industry [27], performed by the Production Engineering Department of Isuzu Motors Ltd., revealed the high efficiency of the aforesaid method and enabled its application. The material used in the tests was steel 34CrMo4 (EN 1.7220, ASTM A1031 Grade G41300). The tests involved the application of the oscillating beam. The beam trajectory is presented in Figure 13.

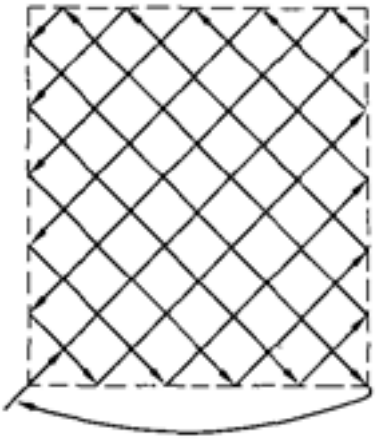

Fig 13. Electron beam deflection pattern based on the Lissajous curve [27]

The first stage of the tests involved the use of the electron beam locally affecting the specimen, examining the result of the aforesaid influence in relation to its time and investigating the effect of electron beam current changes on the depth of the hardened layer. During the tests it was possible to notice that the specimens with the melted material (on the surface) contained cracks. In relation to applied parameters, the maximum hardening depth without the presence of the liquid phase amounted to 0.9 mm. The results of the tests were sufficiently satisfactory to take a decision to use the electron beam welding process to harden the tappets of an Isuzu B6 engine. The electron beam can be used to harden surfaces of elements having complicated shapes (such as the aforesaid tappets). The shape of the tappet contact surface is too complex to be hardened using the induction method. Figure 14 presents a diagram showing the distribution of hardness in an Isuzu B6 engine tappet subjected to electron beam hardening.

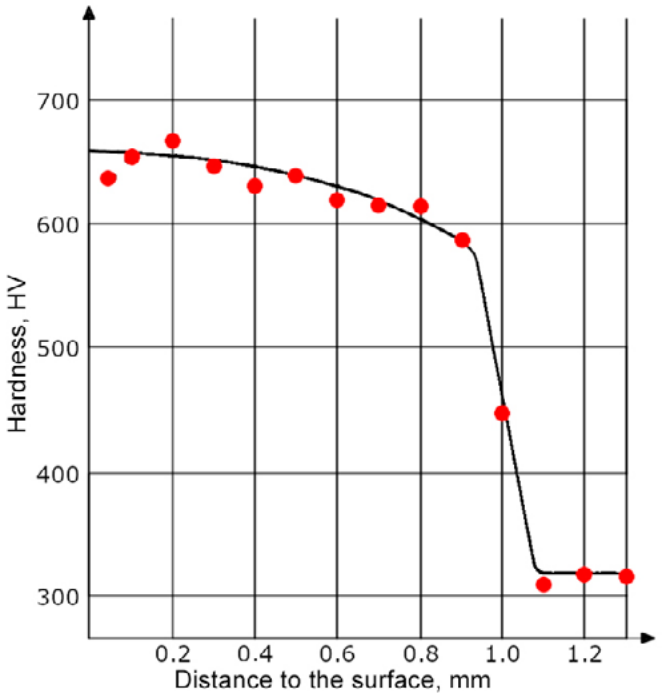

Fig. 14. Hardness distribution in the Isuzu B6 engine tappet [27]

Abrasive wear resistance tests revealed that the wear of the element was reduced by half. Because process-related deformations were very small, the electron beam hardening technology was, with similar results as in the aforesaid case, applied to harden the contact surface of the clamping ring in the gearbox synchroniser.

The authors of publication [28] used the electron beam hardening process to reconstruct turbine blades. The refurbishment process involved grinding off eroded stellite layers. Afterwards, the specimens were subjected to the electron beam hardening process aimed to obtain the martensitic structure and, consequently, improve the abrasive wear resistance of the material surface layer. The manipulator of a workpiece (processed in an EB ESA 150-MR machine) was supplement with a manually operated blade positioning device. As a result, after adjusting appropriate parameters, the hardening of the blade on the leading edge only required two runs, whereas that on the trailing edge – only one run. The electron beam

hardening process enabled the obtainment of surface hardness restricted within the range of 700 HV0.03 to 800 HV0.03, which, in turn, made it possible to continue the effective use of the element. According to the authors, the cost of the process constituted a mere 1/15 of the cost required to make a new blade.

Electron beam hardening could also include the obtainment of the liquid phase during the process. During tests discussed in publication [29], the use of the electron beam hardening technology made it possible to increase the hardness of the melted layer by as many as 300 HV (in relation to the base material) and, in addition, to smoothen the surface subjected to processing. The material used in the above-named case was steel 30CrMnSiA (PN 30HGSA). The specimen was locally affected by the electron beam applied in the oscillating square-shaped mode; the length of the square side being 8 mm. The parameter changed during the tests was the time, during which the specimen was affected by the electron beam. An increase in the aforesaid time was accompanied by an increase in the amount of energy supplied to the material surface. Figure 15 presents the dependence of the hardened layer depth and resultant surface hardness on the density of supplied energy resulting from the time, during which the specimen surface was affected by the electron beam.

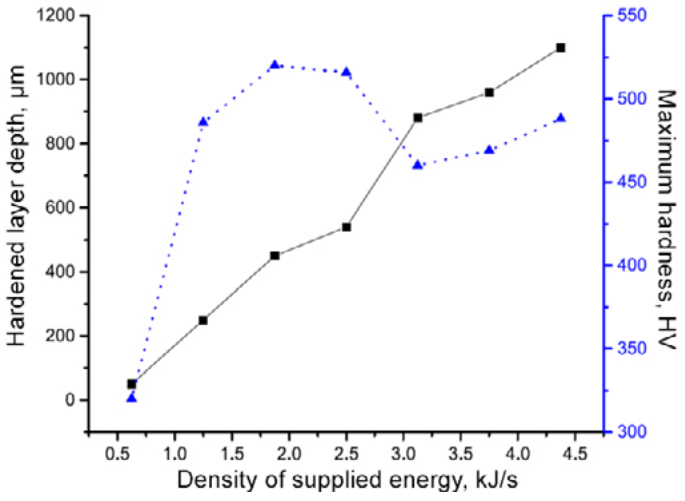

Fig. 15. Dependence of the hardened layer depth and resultant surface hardness on supplied energy density [29]

The surface hardness tests revealed that in terms of the beam effect time exceeding 4 s (corresponding to the density of supplied energy amounting to 2.5 kJ/cm^2), the roughness of the surface started to increase in the linear manner. The optimum results were obtained in relation to the beam effect time restricted within the range of 3 s to 4 s, in relation to which it was possible to observe a decrease in surface roughness restricted within the range of 16.8 nm to 28.7 nm and, at the same time, an increase in hardness from approximately 200 HV to more than 500 HV. The hardening depth was restricted within the range of 0.4 mm to 0.6 mm. Figure 16 presents the correlation between the obtained surface roughness and the time, during which the specimen surface was affected by the electron beam.

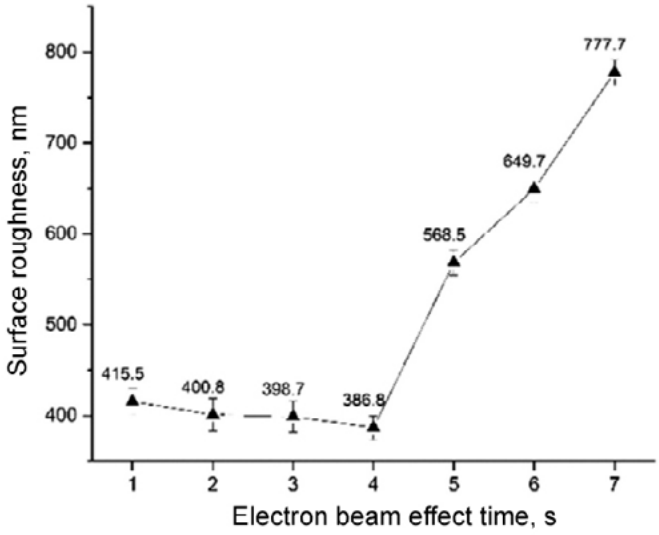

Fig. 16. Correlation between the surface roughness and the time of electron beam effect [29]

Publication [30] presents test results concerning the process involving the electron beam hardening and melting of steel 40CrMn (ISO 41Cr4) containing 0.41% C, 1.02% Mn, 0.25% Si, 1.10% Cr, 0.014% P, 0.013% S and 0.015% Ni. The electron beam oscillating trajectory was in the form of a circle having a 7 mm long diameter. The tests also involved the use of an accelerating voltage of 60 kV, a current of 4 mA, a hardening rate of 300 mm/min and an oscillation frequency of 200 Hz. The hardening process consisted

in the making of three parallel beads with various gaps (overlaps) between them. The calculated values of the gap between the beads, i.e. 4.69 mm, 3.15 mm and 1.05 mm, corresponded to an overlap of 33%, 55% and 85% of the entire bead width respectively. The processing of the surface made it possible to increase hardness up to approximately 650 HV; the base material hardness being 300 HV. Because of the interaction of the thermal cycles of the subsequent beads, it was possible to observe the tempering phenomenon in the preceding beads. The hardness in the tempered zone dropped to approximately 400 HV. The multi-bead specimen with the smallest overlap (33%) was characterised by the highest uniformity of hardness distribution on the surface. The hardening process made it possible to increase the abrasive wear resistance of the specimens by nearly twice.

The authors of publication [31] performed tests involving the electron beam hardening of steel 5CrMnMo (EN 35CrMo7, DIN 40CrMnMo7, 1.2311). The electron beam oscillating trajectory was in the form of a circle having a 10 mm long diameter. The tests also involved the use of an accelerating voltage of 70 kV, an oscillation frequency of 300 Hz, a travel rate of 60 mm/min and electron beam current (changeable parameter) restricted within the range of 6 mA to 8 mA. It was demonstrated that the continuous scanning electron beam (CSEB) method significantly affected the morphology of the surface. First, along with an increase in electron beam current, it was possible to observe a gradual increase in the bead depth. Also, initially, an increase in current was responsible for the improvement (i.e. reduction) of surface roughness. In relation to a current of 7 mA it was possible to reduce surface roughness from 2.23 μm to 0.90 μm. Because of the surface tension, the molten metal flowed down to the lower areas of the surface. As a result, the surface of the materials subjected to processing became significantly smoother. Because of an increase in the temperature of the melted zone, a further increase in current resulted in a decrease

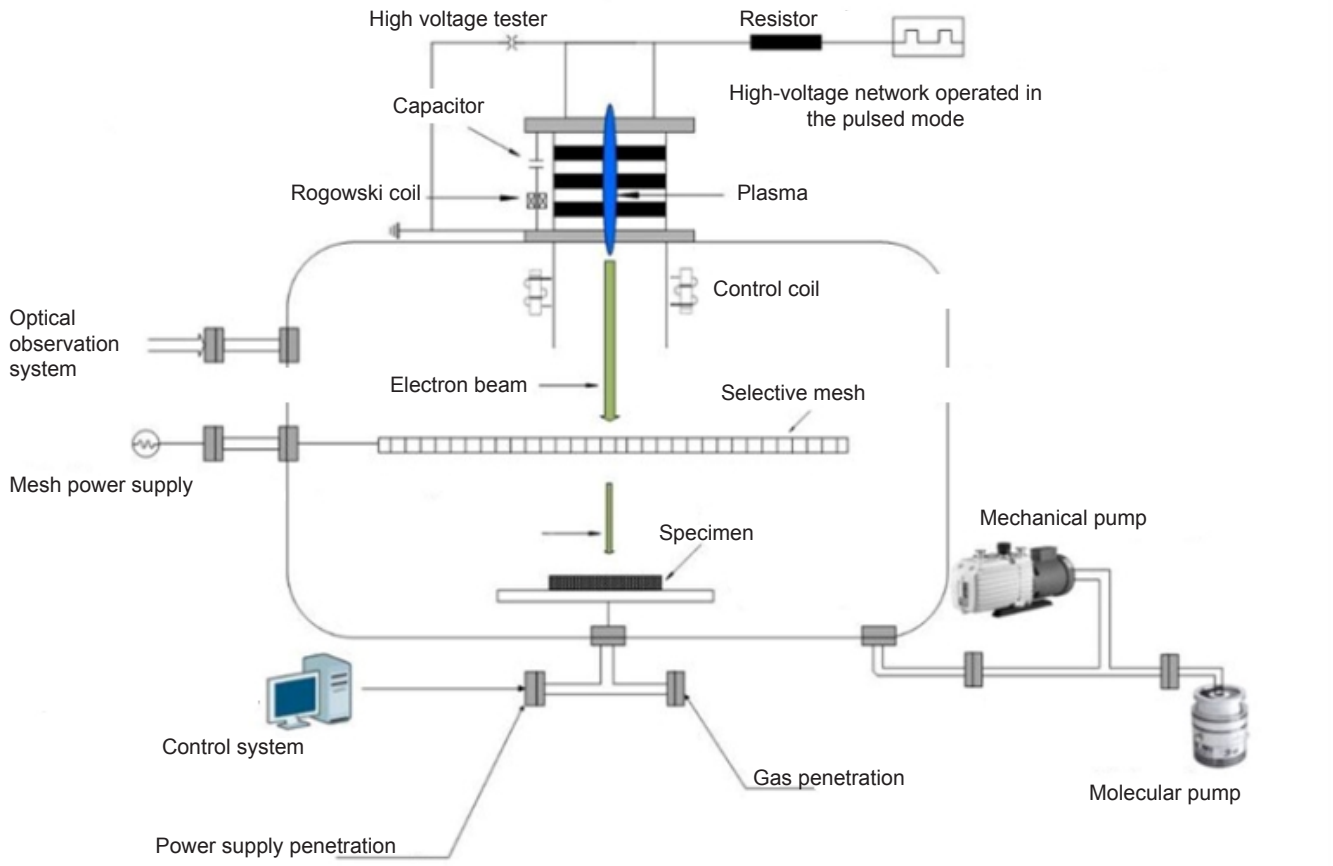

Fig. 17. Schematic diagram of the pulsed electron beam machine featuring pseudospark discharge [33]

in the surface tension of the liquid metal, which, in turn, resulted in the reduction of surface roughness. When the electron beam current amounted to 8 mA it was possible to observe the formation of craters on the specimen surface. The formation of the above-named craters resulted from the partial evaporation of non-metallic inclusions. In comparison with the initial state, the microhardness of the surface improved noticeably, growing along with an increase in electron beam current and reaching its optimum value when current amounted to 7 mA. The maximum hardness amounted to 656 HV, whereas the hardness of the base material was 355 HV.

The electron beam processing of material surface can be performed not only using continuous but also pulsed electron beam operation. The application of high-current pulsed electron beam (HCPEB) devices enables the obtainment of heating rates higher than those typical of machines where the electron beam operation is continuous. Depending on the source, the maximum obtainable heating rates of HCPEB machines are restricted within the range of 10^8 K/s to 10^9 K/s, whereas those typical of the CEB/CSEB method are restricted within the range of 10^5 K/s to 10^6 K/s [10, 12, 18]. An exemplary schematic diagram of the HCPEB machine is presented in Figure 17.

Recent years have also seen tests concerning surface processing methods involving the use of the pseudospark discharge technique, characterised by the ability to quickly initiate and terminate plasma (facilitating the obtainment of high energy increase rates). The above-named technique enables the fast, stable and repeatable performance of the process. Machines using pseudospark discharge (Fig. 17) are designed as pulsed electron beam sources characterised by the short duration of impulses (from tens to hundreds nanoseconds), high peak energy (from hundreds to tens of thousands electronvolts) and high electron beam current (from tens to thousands amperes) [32, 33].

Publications [33, 34] present results of tests involving the use of the pulsed electron beam processing on the structure and properties of the surface layer. The material used in the tests was steel AISI 1045 containing 0.45% C, 0.31% Si, 0.58% Mn, 0.010% P and 0.018% S. The tests also involved the use of an accelerating voltage of 5 kV, a discharge current of 1 kA, an impulse duration of 100 ns and a beam effect radius of 5 mm. The specimen was exposed to 1000 impulses and, next, subjected to inspection. The SEM (scanning electron microscopic) and XRD (X-ray diffractometric) tests enabled the precise identification of phases formed on the surface layer. The electron beam effect was responsible for the partial melting of the surface (to a depth of 2 μm) and structural changes reaching a total depth of 6 μm (from the surface). The specimens processed by the electron beam were characterised by significant grain refinement. In addition, it was possible to observe the formation of the amorphous phase on the specimen surface as well as the formation of the metastable austenite phase. The average grain size in the melted zone amounted to 0.34 μm, whereas that in the heat affected zone amounted to 0.23 μm. The melted zone boundary as well as the specimen surface were characterised by the presence of significant roughness, implying non-uniform heating, and, consequently, the non-uniform melting of the material surface.

The application of the pulsed electron beam in the hardening of tool steel AISI D2 is presented in publication [35]. The tests presented in the aforesaid publication involved the use of a Nadiezhda-2 device, generating the high-current pulsed electron beam (HCPEB). The above-named device is capable of generating the electron beam having energy restricted within the range of 10 keV to 40 keV, an impulse duration of approximately 1 μs and energy density restricted within the range of 0.5 J/cm^2 to 5 J/cm^2 as well as obtaining the cross-sectional area restricted within the range of 10 cm^2 to 50 cm^2.

The specimens were subjected to hardening performed using constant parameters and the changeable number of impulses affecting the specimen surface. When the number of impulses was low, the non-metallic inclusions were responsible for the formation of craters on the element surface. In relation to such a high number of impulses, most carbides in the surface layer were dissolved, leading to the formation of more homogenous layers. The microstructure of the molten layers was composed of fine-grained austenite and precipitates of carbides; the size of carbide grains did not exceed 150 nm. In spite of a high cooling rate of 10^7 K/s, significantly exceeding the critical rate, the martensitic transformation did not take place. The martensitic transformation is known to significantly depend on the state of the austenitic phase. In the case under discussion, the phase was formed directly during fast solidification. The fact that the phase contained dissolved Cr and C significantly increased its strength. The high degree of grain refinement directly affected the stabilisation of phase γ. Because of the greater obstacle to martensitic phase nucleation, the transformation of the above-named phase into martensite was impeded. In addition, the tests did not reveal the presence of dislocations within fine-grained austenite particles, whereas such presence facilitates the nucleation of the martensitic phase. The combination of the above-presented factors was responsible for the possible drop of the Ms point below room temperature, thus precluding the martensitic transformation.

Summary

Electron beam surface hardening can be applied in the fabrication of a wide range of elements characterised by abrasive wear resistance such as cutting tools, work surfaces of toothed gears, elements of shafts or bearings, etc. The electron beam hardening process is primarily used in the production of elements characterised by complicated geometry, and elements, the surface of which must be heated very fast or very precisely. The electron beam hardening method enables the obtainment of hardened layers, the thickness of which can be restricted within the range of single micrometres to a few millimetres. Electron beam hardening machines can work in the continuous or pulsed modes and be used to fabricate melted layers or layers without the liquid phase. In terms of surface layers subjected to hardening, electron beam processing enables the obtainment of a hardness of as many as 1400 HV0.1.

Acknowledgements

The overview of reference publications was performed within the project entitled *Innovative Technology of Making Wear-Resistant Coatings Based on the Nanostructurisation of the Surface Layer*; agreement no. TECHMATSTRATEG-III/0028/2019-00, financed by the National Centre for Research and Development.

References

[1]Vanpaemel J.: History of the hardening of steel: science and technology. Journal de Physique Colloques, 1982, vol. 43, no. C4, pp. 847–854.

[2] Schubert H.: History of British Iron and Steel Industry c.450 BC to AD 1775. 1957.

[3] A. den Ouden: The Production of Wrought Iron in Finery Hearths. Historical Metallurgy, 1981, vol. 15, no. 2, pp. 63–87.

[4] Burakowski T., Wierzchoń T.: Inżynieria Powierzchni Metali. Wydawnictwo Naukowo-Techniczne, Warszawa 1995.

[5] Dobrzański L.A. : Materiały inżynierskie i projektowanie materiałowe. Podstawy nauki o materiałach i metaloznawstwo. Wydawnictwo Naukowo-Techniczne, Warszawa 2006.

[6] Nowotyńska I., Kut. S.: Wybrane metody obróbki powierzchni narzędzi do formowania metali. Logistyka 6/2014.

[7] Dobrzański L.A., Dobrzańska-Danikiewicz A.D.: Obróbka powierzchni materiałów

inżynierskich. Open Access Library, 2011, vol. 5.
[8] Pawłowski B.: Obróbka cieplna i cieplno-chemiczna stali. Praca zbiorowa pod redakcją J. Pacyny: Metaloznawstwo. Wybrane zagadnienia. Uczelniane Wydawnictwo Naukowo-Dydaktyczne AGH, Kraków 2005, pp. 175–202.
[9] Jankowski T., Głowacka M.: Hartowanie i odpuszczanie stali węglowych. Praca zbiorowa pod redakcją J. Hucińskiej: Metaloznawstwo. Materiały do ćwiczeń laboratoryjnych. Wydawnictwo Politechniki Gdańskiej. 1995, pp. 107–129.
[10] Valkov S., Ormanova M., Petrov P.: Electron-Beam Surface Treatment of Metals and Alloys: Techniques and Trends. Metals, 2020, vol. 10, 1219.
[11] Ribton C.: Intelligent power supplies for electron beam welding at 300 kV and 150 kW. IEE Colloquium on Power Electronics for Demanding Applications (Ref. No. 1999/059), 1999, pp. 4/1–4/7.
[12] Pilarczyk J., Węglowski M.S.: Spawanie wiązką elektronów. Welding Technology Review, 2015, vol. 87, no. 10.
[13] Węglowski M.S., Jachym R., Krasnowski K., Kwieciński K., Pikuła J., Śliwiński P.: Electron Beam Melting of Thermally Sprayed Layers – Overview. Biuletyn Instytutu Spawalnictwa, 2021, no. 3, pp. 7–19
[14] https://www.ebpglobal.com/
[15] https://commons.wikimedia.org/
[16] Angelov V., Ormanova M., Kaisheva D., Lazarova R., Dimitrova R., Petrov P.: Selective electron beam surface alloying of aluminum with TiCN nanoparticles. Nuclear Instruments and Methods in Physics Research. B 2019, no. 440, pp. 88–94.
[17] Panin A., Kazachenok M., Perevalova O., Martynov S., Panina A., Sklyarova E.: Continuous Electron Beam Post-Treatment of EBF3-Fabricated Ti–6Al–4V Parts. Metals, 2019, no. 9, pp. 699.
[18] Dossett J., Totten G.E.: Steel Heat Treating Fundamentals and Processes. Introduction to Surface Hardening of Steels. ASM Handbook, Vol. 4A. Revised by Michael J. Schneider, The Timken Company, and Madhu S. Chatterjee, 2013.
[19] DVS Technical Codes on Electron Beam Welding. English Edition. 2013. Vol. 8. ISBN 978-3-87155-244-1.
[20] Klaus-Rainer Schulze: Electron Beam Technologies. Wissen kompakt. 2012, DVS Media, ISBN 3-87155-227-5.
[21] https://www.pro-beam.com/en/contractmanufacturing/hardening/.
[22] Matlák J., Dlouhý I.: Properties of Electron Beam Hardened Layers made by Different Beam Deflection. Manufacturing Technology, 2018, no. 18, pp. 279–284.
[23] Petrov P. – Optimization of carbon steel electron-beam hardening J. Phys.: Conf. Ser. 223 012029. 2010.
[24] Friedel K.P., Felba J., Wymyslowski A., Pobol I.: A systematic method for optimizing the electron beam hardening process. Vacuum, 1996, vol. 47, no. 11, pp. 1317–1324.
[25] Song R.G., Kepeng Z., Guangliang C.: Electron beam surface treatment. Part I: surface hardening of AISI D3 tool steel. Vacuum, 2003, no. 69, pp. 513–516.
[26] Dimitrov D., Aprakova M., Valkanov S., Petrov P.: Electron beam hardening of ion nitrided layers. Vacuum, 1998, vol. 49, no. 3, pp. 239–246.
[27] Katsuyuki M, Shiroh M., Takayuki H., Masahiko K.: Electron beam hardening. International Journal of Materials and Product Technology, 1990, vol. 5, no. 3.
[28] Storch W., Mühl F., Schulze K.R.: Electron beam hardening for the regeneration of turbine blades. Welding International, 1988, vol. 2, no. 12, pp. 1127–1130.
[29] Yulei F., Jing H., Xianfeng S., Yingying W., Wansheng Z.: Surface hardening of 30CrMnSiA steel using continuous electron beam. Nuclear Instruments and Methods in Physics Research, Section B:

Beam Interactions with Materials and Atoms, 2017, no. 410, pp. 207–214.
[30] Jie Y., Rong W., Deqiang W., Chenggong M., Hui W.: Effect of different scanning modes on the surface properties of continuous electron beam treated 40CrMn steel. Nuclear Instruments and Methods in Physics Research Section B: Beam Interactions with Materials and Atoms, 2020, vol. 467, pp. 102–107.
[31] Deqiang W., Xiaobing W., Rong W., Hongyang C.: Surface modification of 5CrMnMo steel with continuous scanning electron beam process. Vacuum, 2018, vol. 149, pp. 118–123.
[32] Weijie H., Jing H., Xiaotong C., Wansheng Z.: Experimental investigations of nanosecond-pulse electron beam profile for metal surface treatments. Materials from 20th Conference on electro physical and chemical machining. Published by Elsevier B. V. 2020.
[33] Yulei F., Jing H., Wansheng Z., Fujun P., Weijie H., Xiaotong C.: Microstructure modification of AISI1045 steel induced by high-current pulsed pseudospark electron beam. Procedia CIRP. 95, pp. 972–975.
[34] Yulei F., Jing H., Xianbing Z., Weijie H., Xiaotong C., Wansheng Z.: Surface modification of AISI 1045 steel by pseudospark based pulsed electron beam. Nuclear Instruments and Methods in Physics Research, B, vol. 434, pp. 88–92.
[35] Zou J.X., Grosdidier T., Zhang K.M., Gao B., Hao S.Z., Dong C.: Microstructures and phase formations in the surface layer of an AISI D2 steel treated with pulsed electron beam. Journal of Alloys and Compounds, 2007, vol. 434–435, pp. 707–709.